Multiband flattening and linear Dirac band structure in graphene with impurities

Multi-band flattening and linear Dirac band structure in graphene with impurities

S. Ahmadkhani,[1] M. Alihosseini,[1] S. Ghasemi,[1] I. Ahmadabadi,[2]
N. Hassani,[1] F. M. Peeters,[3,4] and M. Neek-Amal[1,4,*]

[1] *Department of Physics, Shahid Rajaee Teacher Training University, 16875-163 Lavizan, Tehran, Iran.*
[2] *Joint Quantum Institute, NIST and University of Maryland, College Park, Maryland 20742, USA.*
[3] *Departamento de Física, Universidade Federal do Ceará, 60455-760 Fortaleza, Ceará, Brazil.*
[4] *Departement Fysica, Universiteit Antwerpen, Groenenborgerlaan 171, B-2020 Antwerpen, Belgium.*

Flat-band in the energy spectrum have attracted a lot of attention in recent years because of its unique properties and promising applications. Special arrangement of impurities on mono-layer graphene are proposed to generate multi-flat bands in the electronic band structure. In addition to the single mid-gap states in the spectrum of graphene with low hydrogen density, we found closely spaced bands around the Fermi level with increasing impurity density which are similar to discrete lines in the spectrum of quantum dots, as well as the unusual Landau level energy spectrum of graphene in the presence of a strong magnetic field. The presence of flat-bands crucially depends on whether or not there are odd or even electrons of H(F)-atoms bound to graphene. Interestingly, we found that a fully hydrogenated (fluoridated) of a hexagon of graphene sheet with six hydrogen (fluorine) atoms sitting on top and bottom in consecutive order exhibits Dirac cones in the electronic band structure with a 20% smaller Fermi velocity as compared to the pristine graphene. Functionalizing graphene introduces various C-C bond lengths resulting in non-uniform strains. Such a non-uniform strain may induce a giant pseudo magnetic field in the system, resulting in a quantum Hall effect.

I. INTRODUCTION

One of the most intriguing topics of condensed matter physics is the emergence of a flat-band (FB) in the electronic band structure of 2D-materials [1–7]. The quenched kinetic energy of electrons due to FB near the Fermi level, promotes interactions between electrons, and facilitates charge transfer between the substrate and adsorbent [8–10]. These FBs demonstrate exclusive properties, such as narrow width, large effective mass of electrons, very high photoemission intensity, large electron-phonon coupling, and sharp density-of-state (DOS) peaks near the Fermi level. Systems containing FBs in their electronic band structure exhibit interesting properties including superconductivity [11], emergent ferromagnetism [12], quantized magnetotransport [13], etc.

There are different ways to manipulate electronic band structure and introduce a FB into 2D-materials, such as by introducing defects [14] and impurities such as hydrogen (H) [15–17], oxygen (O) [18, 19], hydroxyl (OH) [16, 18, 19], fluorine (F) [17, 20], and adsorption of NO molecule [21]. It was found that covalently bound impurities, such as hydroxyl groups, can induce midgap states in graphene [16, 17]. For instance, it is also known that insertion of alkali and alkaline earth metals into 2D-materials can increase the carrier concentration and DOS at the Fermi energy [22, 23]. FBs can especially be studied by angle-resolved photoemission spectroscopy (ARPES). For example, the FBs in 1T-VSe_2 and five-layer graphene on the deposited 3C-SiC was studied using ARPES [24, 25].

The most well-known example of real 2D dimensional materials with FB (or almost FBs) is the magic-angle twisted bilayer graphene [26, 27]. Here the formation of a FB is accompanied by a broad variety of strongly-correlated effects and electronic phase transitions, including unconventional superconductivity [28, 29]. Another example is a single layer of InSe where a nearly flat hole band appears without twisting. The appearance of this band is associated with an atypical strong electron-phonon interaction and proximity to ferromagnetic and charge-density-wave instabilities [30]. In addition to defected graphene, graphene with impurities can have FBs in their electronic spectrum [31–33].

A graphene based counterpart completely functionalized by hydrogen atoms [34], i.e., graphane, is a simple case to study the effect of impurities and their arrangement on electronic properties. Graphane was theoretically investigated by Sofo and coworkers [35] and later experimentally realized by Elias *et al.* [36]. In graphane compared to graphene, carbon hybridization is changed from sp^2 to sp^3, resulting in an insulator with a band gap of 4 eV [37–39]. Also, it is demonstrated that partially hydrogenated graphene is a semiconductor with variable band gaps [15, 39]. Therefore, the C/H ratio and the distribution of H atoms on hydrogen-functionalized graphene are important factors that can affect its electronic properties such as conductivity and electronic band structure [38, 40]. For example, recently, Li *et al.* showed that there are two non-trivial isolated FBs that appear around the Fermi level for a graphene containing a special arrangement of hydrogens [41]. Interestingly, their introduced isolated FBs are similar to those they have found for the interlocking-circles lattice. In most cases, FBs are located in a small part of the reciprocal lattice which appear as a consequence of special

* mehdi.neekamal@gmail.com

lattice geometry and destructive quantum interference.

In this paper, we focus on the physics of graphene mono-layer (MLG) having different functional groups such as H, OH, and F. By using density functional theory (DFT) calculations we systematically investigated the electronic band structure and the effect of distribution of the functional groups (O, F) on the electronic properties of graphene. Hydrogenated structures are presented in the main text, whereas the results of other functional groups are reported in the supplementary information (SI) file. In particular we report on multi-flat bands, uncrossing (isolated) bands and Dirac like bands for hydrogenated (fluorinated) graphene. Also despite the common believe, in the last part of our work, we show that adding guest atoms do not necessarily destroy the Dirac cone in the spectrum of graphene.

II. COMPUTATIONAL DETAILS

First-principles calculations are performed to study the electronic properties of hydrogenated and fluorinated graphenes. The GGA approximation with the PBE exchange-correlation functional are used for all calculations as implemented in the Quantum ESPRESSO package. The cut-off for plane-wave kinetic energy and charge density is taken to be 50 Ry and 500 Ry, respectively. Total energy convergence threshold is set to be 10^{-6} eV. A vacuum of 15 Å is inserted along z-axis to eliminate interactions between graphene layer's images in the presence of periodic boundary condition (PBC). After convergence test, a $6 \times 6 \times 1$ **k**-point mesh with Gaussian smearing of 0.01 Ry is used for the Brillouin zone (BZ) integration in wave-vector space in all of our simulations except for the non-self-consistent calculations.

In studying the electrical conductivity, Boltzmann theory [42–44] is an appropriate tool to gain insight into the transport properties of real materials. In this theory, the electric current is expressed in terms of the conductivity tensor and group velocity in the presence of the electric and magnetic fields, which altogether results in conductivity tensor. The BoltzTraP package, is used to calculate the conductivity tensor. This program calculates semi-classical transport based on all electrons pseudo potential which applies linearly augmented plane wave method within the framework of the Quantum ESPRESSO package. Also, an energy broadening of 0 meV is used in the calculations.

III. RESULTS AND DISCUSSION

A. A midgap state

Different configurations of functionalized MLG with various functional groups provide remarkable band structure with unique properties. As a standard example, when a hydrogen atom is absorbed [32], one of the unpaired electrons in the resonance structure forms a new bond with a hydrogen atom, and the other remains unpaired (see Fig. 1(a)). The latter electron is delocalized on a broader lattice area. In general, by H-chemisorption of carbon atoms, the hybridization remains sp^2. Here, we considered other conditions which can lead to sp^3 hybridization and a possible gain in the chemisorption of the impurities. Here, we revisit functionalized graphene with hydrogen and other functional groups that result in several split and semi-parallel FBs emerging in the spectrum. Figure 1 illustrates the well-known and simplest feasible scenario in which a hydrogen atom is added to MLG, resulting in a FB close to the Fermi level. The green spheres in the left panels of Fig. 1 represent carbon atoms, and the red sphere indicates a carbon atom that is bound to a hydrogen atom on top of the MLG. In fact, when a hydrogen atom binds to a carbon atom, the π bond of the adjacent carbon atoms are broken and the corresponding electrons participate in the formation of C-H bond and the appearance of a FB at the Fermi level.

The electronic conductivity presented in the right panel of Fig. 1(b) is zero in the gap region. The midgap state of zero energy does not contribute to conduction. Other structures having different functional groups and similar electronic band structures are given in the SI.

The formation of C-H bond changes the hybridization of carbon atom from sp^2 to sp^3. As seen in Fig. 1(c and d) the lowest unoccupied crystal orbital (LUCO) and the highest occupied crystal orbital (HOCO) illustrate the distribution of electrons on each atom. The electron distribution in HOCO is concentrated on the hydrogen atom, but in LUCO, it is dispersed throughout the carbons around the hydrogen atom. The transformation of carbon sp^2 hybridization in pristine graphene to the sp^3 hybridization in functionalized graphene causes a change in the bond lengths and corresponding angles [34].

The normal C-C bond length is 1.42 Å in graphene and graphite, and the standard bond angle is 120°. For sp^3 hybridization, the C-C bond length is 1.54 Å, angle is 109.5°, and the C-H bond length is 1.086 Å. One can see in Table I that for single hydrogen atom the C-H bond length is not close to the standard value, and C-C-H and C-C-C angles are between 104.6°- 110.5° and 107.8°- 120°, respectively. Also, the C-C bond length lies in the range 1.42 Å - 1.54 Å. This implies intermediate character of hybridization between sp^2 and sp^3.

B. Midgap state and uncrossing bands

By increasing the number of impurities we will show that different arrangement of functional groups influence the electronic band structure significantly, e.g, a band gap is induced in the band structure, shifting electronic characteristics transits from metal to semiconductor. For instance, as can be seen in Fig. 2 (a), there is a gap in

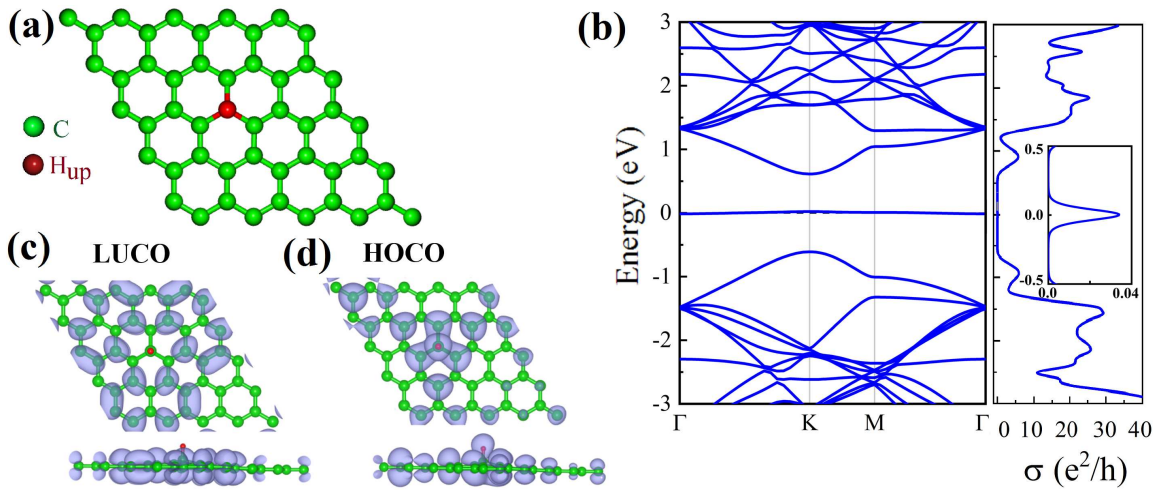

Figure 1. (a) Partially functionalized graphene with one hydrogen atom in 5×5 computational unit cell and (b) left: corresponding electronic band structure, and right: electronic conductivity. The inset is a zoom-in of the electronic conductivity around the Fermi level. (c and d) Electron distribution of LUCO (lowest unoccupied crystal orbital) and HOCO (highest occupied crystal orbital), with a top and side views.

Table I. The bond lengths of functionalized graphene with different number of hydrogen atoms corresponding to the figures. Significant changes happens in the C-C-H and C-C-C (n) angles. Here, "n" and "f" represent the next and far from the functionalized region, respectively. C^H refers to a carbon atom bonded to a hydrogen atom. The used cell in the calculations is 5×5 which contains 50 carbon atoms.

#H	**C-C(f)**	**C-C(n)**	**C^H-C**	**C^H-C^H**	**C-H**	**∠CCH**	**∠CCC(n)**	**∠CCC(f)**
1 (Fig. 1(a))	1.42	1.40	1.50	–	1.12	104.60	114.12	119.74
2 (Fig. 2(a))	1.42	1.41	1.50	1.52	1.12	106.86	110.76	120.36
5 (Fig. 2(e))	1.42	1.37	1.50	1.54	1.12	107.47	108.00	119.82
6 (Fig. 5(a))	1.42	1.40	1.49	1.52	1.11	108.07	108.13	120.28
9 (Fig. 3(a))	1.42	1.40	1.50	1.53	1.11	109.56	108.80	119.94
30 (Fig. 3(e))	1.42	1.41	1.48	1.50	1.10	110.44	107.85	120.04
46 (Fig. 4(e))	–	–	1.47	1.50	1.13	105.02	111.13	–
47 (Fig. 4(c))	–	–	1.47	1.52	1.11	106.63	112.59	–
48 (Fig. 4(a))	–	–	1.47	1.51	1.11	106.42	110.38	–

the symmetrical electronic band structure when two hydrogen atoms are added on top and bottom of carbon atoms. By adding one more hydrogen atom, two uncrossing bands appear around the Fermi level and one FB emerges at the Fermi level.

In general odd number of adsorbed H-atoms provides a midgap state. As an example, five hydrogen atoms on a carbon hexagon leads to the emergence of a FB at the Fermi level (see Fig. 2 (f)). This FB occurrence is independent of the distance of the hydrogenated carbon atoms from each other, e.g., for three carbon atoms near and far from each other, a FB emerges at the Fermi level (see Fig. S1 (a, b)). This is also valid for removing an odd number of hydrogen atoms from fully hydrogenated graphene (see Fig. S1 (c, d)).

The electronic conductivity of a functionalized hexagon by two and five hydrogen atoms is presented in the right panels of Fig. 2 (b) and (f), respectively. There is a negligible conductivity at the Fermi level for the structure having two hydrogen atoms on a hexagon while a small peak at the Fermi level is observed for five bonded hydrogen atoms that corresponds to the induced FB. It is shown in Figs. 2 (c,d) that the electron distribution in both HOCO and LUCO is concentrated on the hydrogen atoms.

When five hydrogen atoms are on a hexagon, the electron distribution HOCO is concentrated on the hydrogen atoms, but LUCO is dispersed throughout the carbons around the hydrogen atoms (see Figs. 2 (g,h)). In fact, when an odd number of hydrogen atoms are located on a hexagon ring, this leaves one unpaired electron, resulting in the presence of a FB at the Fermi level.

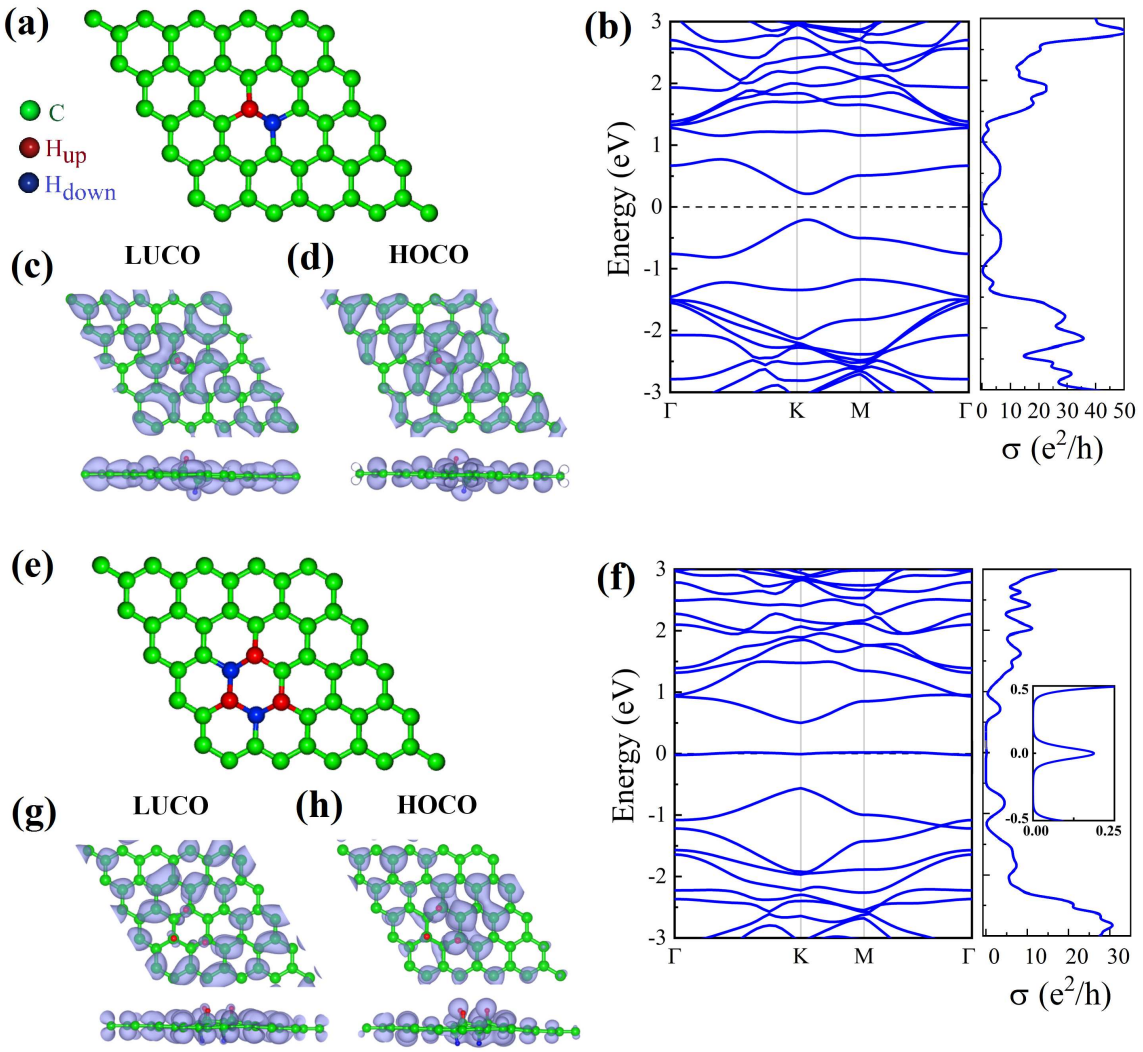

Figure 2. Partially functionalized graphene with (a) two and (e) five hydrogen atoms in 5×5 computational unit cell. (b and f) Left: the symmetrical band structure, and right: electronic conductivity. The inset is a zoom-in of the electronic conductivity around the Fermi level. (c, d, g, and h) Electron distribution of LUCO and HOCO, respectively with top and side view.

C. Several avoided crossing bands

The number of FBs around the Fermi level increases as hydrogen atoms are separated leading to the formation of multi- and semi-parallel bands (see Fig. 3). The aforementioned effect depends on the number of unpaired electrons which are separated from each other. These unpaired electrons induce separate FBs around the Fermi level. By increasing the number of functional groups the number of electronic bands around the Fermi level increases. As shown in Fig. 3(a), by adding nine hydrogen atoms the avoided symmetrical crossing bands around the Fermi level increases (Fig. 3(b)). The corresponding electronic conductivity (right panel of Fig. 3(b)) shows a tiny peak at zero energy corresponding to the induced FBs at the Fermi level.

As the HOCO and LUCO orbitals of this typical configuration in Figs. 3(c,d) show, the electrons are randomly distributed on the sheet due to the odd number of hydrogen atoms. By increasing further the number of hydrogen atoms and arranging them on carbon atoms, bands are much more flattened around the Fermi level (Fig. 3(f)). The electronic conductivity in the right panel of Fig. 3(f) exhibits a significant peak which corresponds to energies around the Fermi level because of emerging of almost parallel FBs. LUCO and HOCO orbitals in Figs. 3(g,h) have complicated pattern and electronic distribution over hydrogen free carbon atoms is larger than for the other atoms.

The bond lengths of different sites vary by increasing the number of functional groups. The bond length variations versus the number of functional groups are listed in Table I. The angles and bond lengths of the carbon atoms close to functional groups are significantly altered

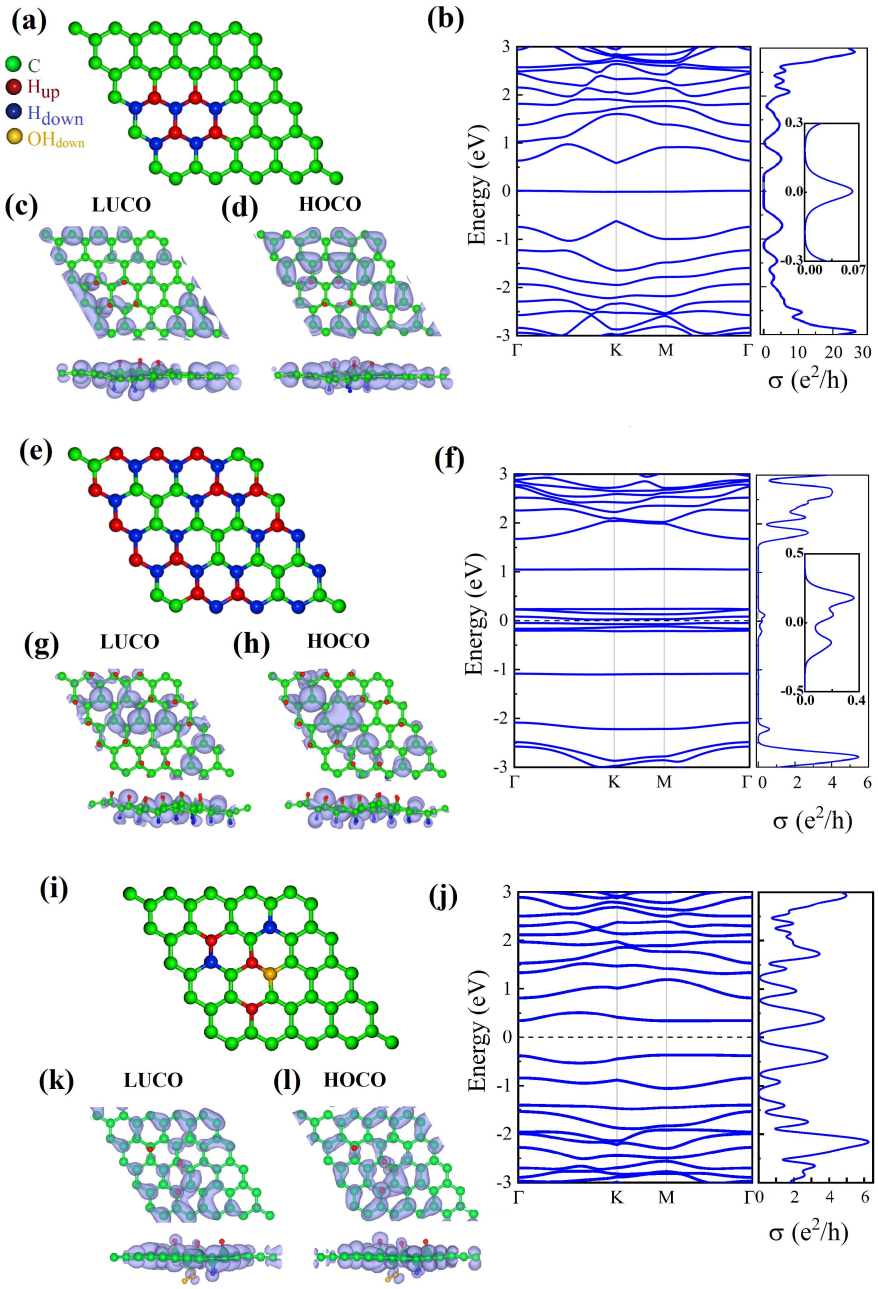

Figure 3. Partially functionalized graphene with (a) nine and (e) thirty hydrogen atoms and (i) one oxygen and five hydrogen atoms in 5×5 computational unit cell. (b, f, and j) Left: corresponding symmetrical (b, j) and multi-parallel (f) electronic band structure, and right: electronic conductivity. The insets are a zoom-in of the electronic conductivity around the Fermi level. (c, d, g, and h) Electron distribution of LUCO and HOCO, respectively with top and side view. The colors of each atom is shown in the legend, at the left-top corner.

compared to those far from the functional groups.

Usually large deformations in graphene can induce strong pseudomagnetic fields [45]. By changing functionalized regions a significant non-uniform strain is induced on the MLG. Consequently, a large pseudo magnetic field can be induced in the system. This is in agreement with the results of Ref. [46], where non-uniform strain distribution in MLG yields giant pseudo magnetic fields causing the emergence of quantum Hall regime . The quantization of energy levels is an important characteristic of the quantum Hall effect, which is observed in the presence of parallel bands around the Fermi level, as shown in Figs. 3 (b,f). Especially the FBs lies in the interval [-300,300] meV around the Fermi level in Fig. 3(f). Surprisingly, two FBs with almost zero width appears at the top and bottom of Fermi level in the energies $\simeq \pm 1$ eV.

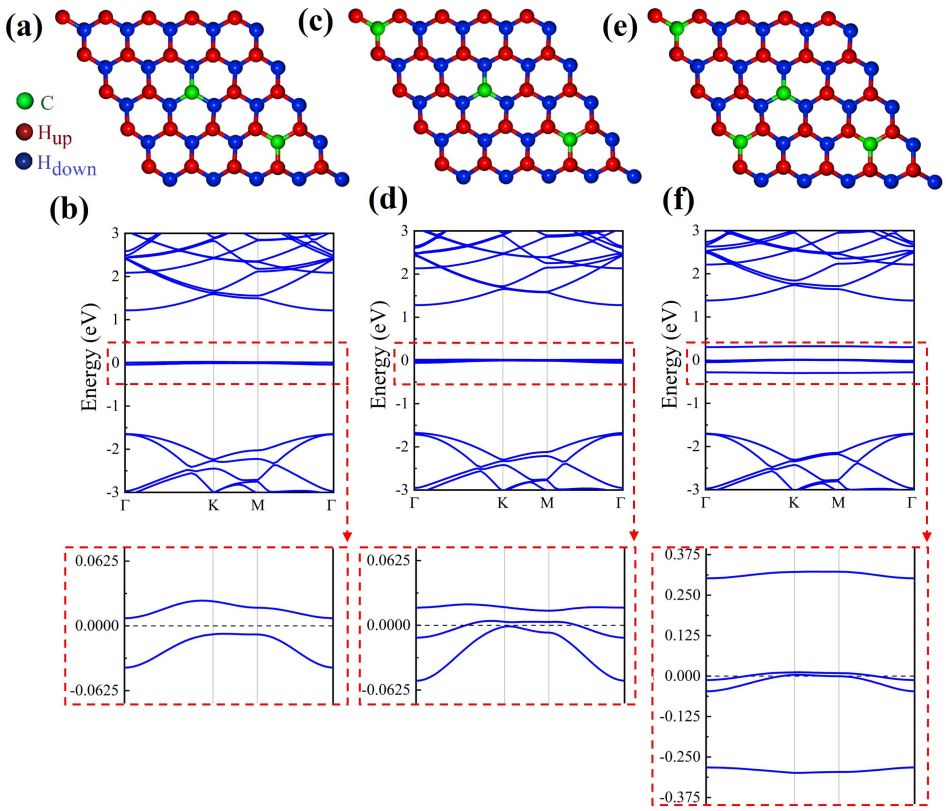

Figure 4. Fully hydrogenated graphene with (a and b) two, (c and d) three, and (e and f) four carbon atoms without any hydrogen atoms. In their electronic band structures multi-flat bands close to the Fermi levels appears. A zoom-in of the bands near the Fermi level is shown in the bottom panels.

As seen from the conductivity curves (right panels of Figs. 3 (b,f)), the peaks relative to FB energies agree with the results reported for the emerging integer quantum Hall effect in silicene subjected to electric and magnetic fields [47]. Another interesting result was found when we added a -OH group in a system having five hydrogen atoms, i.e. Fig. 3(e). The corresponding band structure is shown in Fig. 3(j) which includes several isolated bands located in the wider range around the Fermi level (see Sec. E below).

Compact percolating states close to the Fermi level is demonstrated in Fig. 4, i.e., overlapping bands around the Fermi level. Such property appears in fully hydrogenation of the MLG with random hydrogen removal. The number of quasi-FB at the Fermi level is proportional to the number of missing hydrogen atoms, e.g, for three missed hydrogen atoms, three quasi-FB appear around the Fermi level.

D. Crossing bands at the Dirac point

Now we turn our attention to a special case of hydrogenated (fluorinated) graphene where a Dirac cone in the band structure of graphene with impurity emerges. The common belief is that any kind of adsorption of functional groups over graphene will destroy the Dirac cone nature of the band structure, or split the bands, opens up a gap, and may generate either midgap states or FBs. However, we found that if one hexagon of graphene is fully hydrogenated (fluorinated) the crossing bands feature of pristine graphene and its low energy spectrum remains unchanged and only the Fermi velocity (V_F) is changed. As is obvious from Fig. 5(b), the Fermi velocity (V'_F) is smaller than the standard V_F of pristine graphene, i.e. $V'_F/V_F \approx 0.8$.

In other words, the gap in the band structure is fully closed when hydrogen atoms bond with the carbon atoms of a hexagon of graphene, as illustrated in Fig. 5. Interestingly, for this particular arrangement of impurities, the pure graphene band structure is recovered. As depicted in Fig. 5 (b), the dashed-solid lines in the left panel represent the band structure of the functionalized graphene with six hydrogen (fluorine) atoms. There is a Dirac point at K similar to the pristine graphene electronic band structure. The electronic conductivity is also illustrated in the right panel of Fig. 5 (b).

The C-C bond lengths of the central hexagon are 1.52 Å, the nearest neighbour C-C bonds around the central hexagon are 1.49 Å and the next nearest one are 1.40 Å. The rest of the bonds far from the center have usual length, i.e. 1.42 Å. Therefore the bond lengths

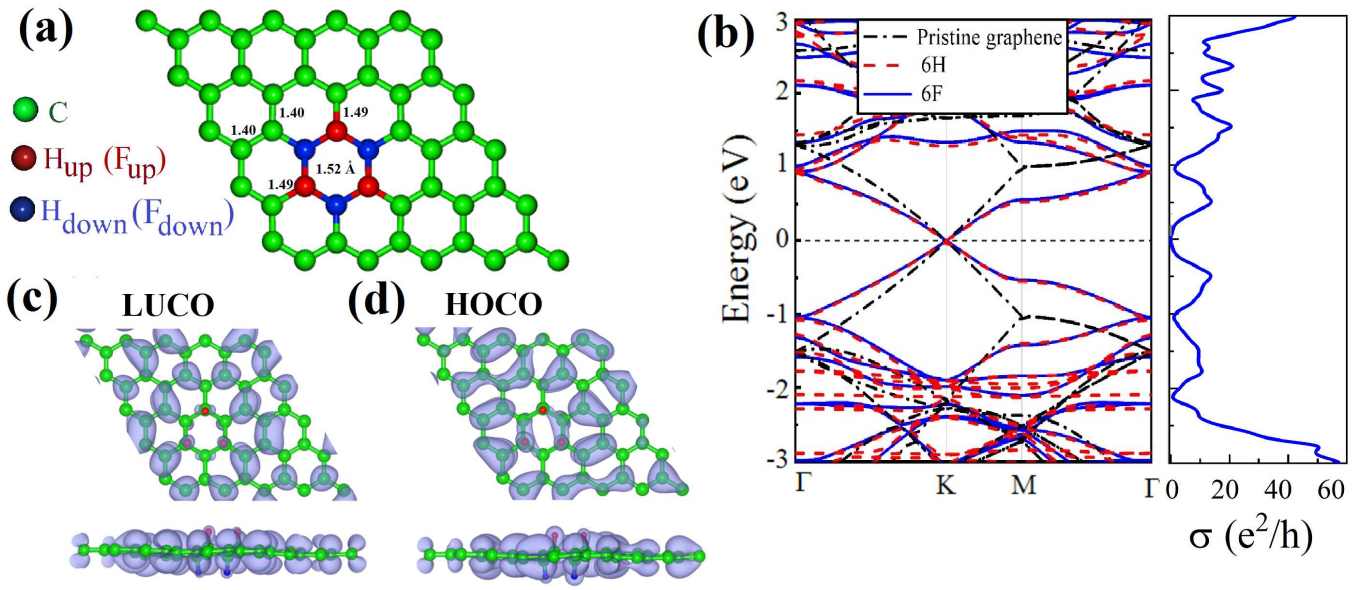

Figure 5. Partially functionalized graphene with six hydrogen (fluorine) atoms that have only on a single hexagon ring. In the caption, carbons functionalized with F and H atoms are represented by the same balls. (b) Left: corresponding electronic band structure (black solid lines), red dashed lines represent pristine graphene electronic band structure (b) Right: represents electronic conductivity. (c and d) Electron distribution of LUCO and HOCO, respectively with top and side view. The C-C bond lengths inside the central hexagon and around it are given close to each bond.

in central and nearest bond lengths are 7% and 5% stretched with respect to the C-C bond lengths in a pristine graphene. Also the difference between two heights of carbon atoms in the A and B-sublattices (containing one up and the other down hydrogen atoms) in the central hexagon is about 0.5 Å which are very close to that of fully hydrogenated graphene (i.e., 0.51 Å) [48].

From orbital properties of the structure, we can observe that LUCO and HOCO are similar to pristine graphene except for regions close to the hydrogen atoms. Notice that the next neighbor hopping between pure carbon atoms around the ring for the graphene hosting a hexagon ring of hydrogens in the origin of the gap-less band diagram is impossible (see Fig. 5). This is due to the fact that the electronic density of HOCO and LUCO orbitals of next neighbor carbon atoms around the hexagon impurity ring do not overlap to create a possible next neighbor hopping.

As is depicted in the electronic density in Fig. 2(b), carbon atoms adjacent to the two carbon atoms with impurity next to each other can have next neighbor hopping. The latter is due to the electronic density overlap between these carbons which is facilitated by the hydrogenated carbon atoms. Since carbon is slightly more electronegative than hydrogen, this overlap is facilitated by more electronic density on the hydrogenated carbon atoms, where they act as a bridge between the next neighbor carbon atoms. Due to the higher electronegativity of fluorine compared to hydrogen and carbon, the hexagon ring hosting fluorine atoms also results in the same gapless system as the next neighbor hopping here, which is even more difficult to happen compared to the hydrogen impurity. However, as seen from Fig. 5(b) the crossing bands for both hydrogenated and fluorinated graphene are almost the same.

It is worthwhile to mention that, applying uniaxial strain on graphene doesn't open a gap [49] which is similar to what happens in this case, i.e a complete symmetry of the induced strain in the system by adsorption of six H or F over a hexagon doesn't either open a gap.

E. Adsorption of other functional groups (O, F)

For other atoms adsorbed on graphene such as O and F in the presence of H atoms, the results are presented in Figs. S2 and S3. As mentioned above, two uncrossing FBs appear around the Fermi level for the structures containing two carbon atoms located far and near from each other while hydrogenated by an H atom (see Figs. 2(a) and S2(a). By adsorbing an O or F atom on the next neighbor carbon atom of two bonded and hydrogenated carbon atoms, the previous two bands disappear and a new nearly FB emerges at the Fermi level. We found that, regardless of the type of functional groups, as the distance between functionalized carbon atoms increases, the number of bands that appear around the Fermi level increases, which is directly related to the number of functional groups. However, as the number of functional groups increases and, consequently, the distance between them decreases, the description of the band structure becomes more complicated. Of particu-

lar interest is the spectrum shown in Fig. 3 (j) where one oxygen and 5 hydrogen atoms are adsorbed and several uncrossing bands are formed in the band structure. It would be worth to mention that such uncrossing bands appear in the solution of standard 1D-potentials such as Kronig-Penney and Mathieu potentials [50]. Moreover, a quantum dot system for the lowest states has parallel bands which are closely spaced around the Fermi level. On one hand, the band structure of the system shown in Fig. 3(j) around the Fermi level is similar to what is seen in the spectrum of a quantum dot system. On the other hand, using scanning tunneling spectroscopy measurement, distinct Landau level spectra and corresponding level-splitting phenomena were observed in graphene layers subjected to strong magnetic field (12 T) [51, 52]. The reported level-splitting phenomena in our work is originated to the change cuased by the added atoms and corresponding bond lengths. The investigation of anomalous quantum Hall effect in our system demands further study. This system can be characterized as a semiconductor with several low energy flat bands with a gap of about 0.8 eV.

IV. CONCLUSIONS

DFT calculations are used to study the electronic properties of partially functionalized graphene. The type and concentration of functional groups influence significantly the physical properties of graphene, by changing the electronic band structure and inducing a band gap, shifting electronic characteristics of graphene from metal to semiconductor. In functionalized graphene, the C-C bond lengths and distribution of impurities in special configurations, has a similar effect as applying non-uniform strains. Such non-uniform strain can induce a large magnetic field [47]. The electronic conductivity peaks associated with these strain-induced parallel bands are identical to those seen in quantum Hall systems under giant pseudo magnetic fields. Adsorbing an odd number of impurities such as H, F, and O in the computational unit cell induces a flat-band (FB) around the Fermi level in the band structure, due to an unpaired electron. Investigation of low unoccupied crystal band orbitals for different hydrogen configurations illustrates how the electronic distribution contributes in forming a FB which are split and uncrossing of bands around the Fermi level. This FB causes a peak in the electronic conductivity. We found that increasing the number of far-distance impurities results in multi-band flattening around the Fermi level. Interestingly, adsorption of six hydrogen and fluorine atoms on a hexagon ring of carbon atoms, reproducing crossing Dirac point at the K-point which is similar to the pristine graphene band structure.

Acknowledgments N. Hassani and S. Ahmadkhani acknowledge ISEF support. We acknowledge fruitful comments and helps by Z. Javdani.

[1] L. Zheng, L. Feng, and W. Yong-Shi, Exotic electronic states in the world of flat bands: From theory to material, Chinese Physics B **23**, 077308 (2014).

[2] D. Leykam, A. Andreanov, and S. Flach, Artificial flat band systems: from lattice models to experiments, Advances in Physics: X **3**, 1473052 (2018).

[3] S. Pathak, T. Rakib, R. Hou, A. Nevidomskyy, E. Ertekin, H. T. Johnson, and L. K. Wagner, Accurate tight-binding model for twisted bilayer graphene describes topological flat bands without geometric relaxation, Physical Review B **105**, 115141 (2022).

[4] L.-H. Tong, Q. Tong, L.-Z. Yang, Y.-Y. Zhou, Q. Wu, Y. Tian, L. Zhang, L. Zhang, Z. Qin, and L.-J. Yin, Spectroscopic visualization of flat bands in magic-angle twisted monolayer-bilayer graphene: coexistence of localization and delocalization, Physical Review Letters **128**, 126401 (2022).

[5] L.-J. Yin, L.-H. Tong, Y.-Y. Zhou, Y. Zhang, Y. Tian, L. Zhang, L. Zhang, and Z. Qin, Direct observation of moiré flat-band breakdown at the edge of magic-angle twisted bilayer graphene, Physical Review B **105**, L201405 (2022).

[6] C. Bao, H. Zhang, X. Wu, S. Zhou, Q. Li, P. Yu, J. Li, W. Duan, and S. Zhou, Coexistence of extended flat band and kekulé order in li-intercalated graphene, Physical Review B **105**, L161106 (2022).

[7] L.-Z. Yang, L.-H. Tong, C.-S. Liao, Q. Wu, X. Fu, Y.-Y. Zhou, Y. Tian, L. Zhang, L. Zhang, M.-Q. Cai, *et al.*, Origami-controlled strain engineering of tunable flat bands and correlated states in folded graphene, Physical Review Materials **6**, L041001 (2022).

[8] D. Wei, C. Zhao, A. Khan, L. Sun, Y. Ji, Y. Ai, and X. Wang, Sorption mechanism and dynamic behavior of graphene oxide as an effective adsorbent for the removal of chlorophenol based environmental-hormones: A dft and md simulation study, Chem. Eng. J. **375**, 121964 (2019).

[9] J.-A. Yan and M. Y. Chou, Oxidation functional groups on graphene: Structural and electronic properties, Physical Review B **82**, 125403 (2010).

[10] J. Tian-Tian, S. Bao-zhen, L. Hua-xiang, L. Yi, and C. Wen-Kai, Binding of hydroxyl and epoxy groups on graphene: Insights from density functional calculations, Chinese J. Struct. Chem. **32**, 1475 (2013).

[11] .

[12] M. Serlin, C. Tschirhart, H. Polshyn, Y. Zhang, J. Zhu, K. Watanabe, T. Taniguchi, L. Balents, and A. Young, Intrinsic quantized anomalous hall effect in a moiré heterostructure, Science **367**, 900 (2020).

[13] S. Wu, Z. Zhang, K. Watanabe, T. Taniguchi, and E. Y. Andrei, Chern insulators, van hove singularities and topological flat bands in magic-angle twisted bilayer graphene, Nature materials **20**, 488 (2021).

[14] M. Vanević, V. M. Stojanović, and M. Kindermann, Character of electronic states in graphene antidot lattices: Flat bands and spatial localization, Physical Re-

view B **80**, 045410 (2009).
[15] H.-C. Huang, S.-Y. Lin, C.-L. Wu, and M.-F. Lin, Configuration-and concentration-dependent electronic properties of hydrogenated graphene, Carbon **103**, 84 (2016).
[16] T. O. Wehling, S. Yuan, A. I. Lichtenstein, A. K. Geim, and M. I. Katsnelson, Resonant scattering by realistic impurities in graphene, Physical Review Letters **105**, 056802 (2010).
[17] T. O. Wehling, M. I. Katsnelson, and A. I. Lichtenstein, Impurities on graphene: Midgap states and migration barriers, Physical Review B **80**, 085428 (2009).
[18] M. Alihosseini, S. Ghasemi, S. Ahmadkhani, M. Alidoosti, D. N. Esfahani, F. Peeters, and M. Neek-Amal, Electronic properties of oxidized graphene: Effects of strain and an electric field on flat bands and the energy gap, The Journal of Physical Chemistry Letters **13**, 66 (2021).
[19] J.-A. Yan, L. Xian, and M. Y. Chou, Structural and electronic properties of oxidized graphene, Physical Review Letters **103**, 086802 (2009).
[20] O. Leenaerts, H. Peelaers, A. Hernández-Nieves, B. Partoens, and F. Peeters, First-principles investigation of graphene fluoride and graphane, Physical Review B **82**, 195436 (2010).
[21] O. Leenaerts, B. Partoens, and F. Peeters, Adsorption of h_2o, nh_3, co, no_2, and no on graphene: A first-principles study, Physical Review B **77**, 125416 (2008).
[22] S. Ichinokura, K. Sugawara, A. Takayama, T. Takahashi, and S. Hasegawa, Superconducting calcium-intercalated bilayer graphene, ACS Nano **10**, 2761 (2016).
[23] K. Tanigaki, T. W. Ebbesen, S. Saito, J. Mizuki, J. S. Tsai, Y. Kubo, and S. Kuroshima, Superconductivity at 33 k in $cs_x rb_y c_{60}$, Nature **352**, 1476 (1991).
[24] T. Yilmaz and E. Vescovo, Revealing flat bands near the fermi level in 1 t- vse 2 by using angle-resolved photoemission spectroscopy, Physical Review B **105**, L041101 (2022).
[25] D. Pierucci, H. Sediri, M. Hajlaoui, J.-C. Girard, T. Brumme, M. Calandra, E. Velez-Fort, G. Patriarche, M. G. Silly, G. Ferro, V. Soulière, M. Marangolo, F. Sirotti, F. Mauri, and A. Ouerghi, Evidence for flat bands near the fermi level in epitaxial rhombohedral multilayer graphene, ACS Nano **9**, 5432 (2015).
[26] E. S. Morell, J. Correa, P. Vargas, M. Pacheco, and Z. Barticevic, Flat bands in slightly twisted bilayer graphene: Tight-binding calculations, Physical Review B **82**, 121407 (2010).
[27] R. Bistritzer and A. H. MacDonald, Moiré bands in twisted double-layer graphene, Proceedings of the National Academy of Sciences **108**, 12233 (2011).
[28] Y. Cao, V. Fatemi, A. Demir, S. Fang, S. L. Tomarken, J. Y. Luo, J. D. Sanchez-Yamagishi, K. Watanabe, T. Taniguchi, E. Kaxiras, *et al.*, Correlated insulator behaviour at half-filling in magic-angle graphene superlattices, Nature **556**, 80 (2018).
[29] Y. Cao, V. Fatemi, S. Fang, K. Watanabe, T. Taniguchi, E. Kaxiras, and P. Jarillo-Herrero, Unconventional superconductivity in magic-angle graphene superlattices, Nature **556**, 43 (2018).
[30] E. Stepanov, V. Harkov, M. Rösner, A. Lichtenstein, M. Katsnelson, and A. Rudenko, Coexisting charge density wave and ferromagnetic instabilities in monolayer inse, arXiv preprint arXiv:2107.01132 (2021).
[31] M. S. de Sousa, F. Liu, F. Qu, and W. Chen, Vacancy-engineered flat-band superconductivity in holey graphene, Physical Review B **105**, 014511 (2022).
[32] T. Wehling, M. Katsnelson, and A. Lichtenstein, Impurities on graphene: Midgap states and migration barriers, Physical Review B **80**, 085428 (2009).
[33] T. Wehling, S. Yuan, A. Lichtenstein, A. Geim, and M. Katsnelson, Resonant scattering by realistic impurities in graphene, Physical review letters **105**, 056802 (2010).
[34] A. A. Dzhurakhalov and F. M. Peeters, Structure and energetics of hydrogen chemisorbed on a single graphene layer to produce graphane, Carbon **49**, 3258 (2011).
[35] J. O. Sofo, A. S. Chaudhari, and G. D. Barber, Graphane: A two-dimensional hydrocarbon, Physical Review B **75**, 153401 (2007).
[36] D. C. Elias, R. R. Nair, T. Mohiuddin, S. Morozov, P. Blake, M. Halsall, A. C. Ferrari, D. Boukhvalov, M. Katsnelson, A. Geim, *et al.*, Control of graphene's properties by reversible hydrogenation: evidence for graphane, Science **323**, 610 (2009).
[37] T. Sreeprasad and V. Berry, How do the electrical properties of graphene change with its functionalization?, small **9**, 341 (2013).
[38] B. R. Matis, J. S. Burgess, F. A. Bulat, A. L. Friedman, B. H. Houston, and J. W. Baldwin, Surface doping and band gap tunability in hydrogenated graphene, ACS nano **6**, 17 (2012).
[39] J. Son, S. Lee, S. J. Kim, B. C. Park, H.-K. Lee, S. Kim, J. H. Kim, B. H. Hong, and J. Hong, Hydrogenated monolayer graphene with reversible and tunable wide band gap and its field-effect transistor, Nature communications **7**, 1 (2016).
[40] M. Jaiswal, C. H. Yi Xuan Lim, Q. Bao, C. T. Toh, K. P. Loh, and B. Ozyilmaz, Controlled hydrogenation of graphene sheets and nanoribbons, ACS nano **5**, 888 (2011).
[41] S. Li, Y. Xie, and Y. Chen, Isolated flat bands in a lattice of interlocking circles, Physical Review B **104**, 085127 (2021).
[42] G. K. Madsen and D. J. Singh, Boltztrap. a code for calculating band-structure dependent quantities, Computer Physics Communications **175**, 67 (2006).
[43] P. Allen, Boltzmann theory and resistivity of metals, Kluwer International Series In Engineering and Computer Science , 219 (1996).
[44] J. M. Ziman, Electrons and phonons: the theory of transport phenomena in solids, Oxford university press , 10 (2001).
[45] M. Neek-Amal and F. Peeters, Strain-engineered graphene through a nanostructured substrate. ii. pseudomagnetic fields, Physical Review B **85**, 195446 (2012).
[46] F. Guinea, M. Katsnelson, and A. Geim, Energy gaps and a zero-field quantum hall effect in graphene by strain engineering, Nature Physics **6**, 30 (2010).
[47] C.-H. Wu, Integer quantum hall conductivity and longitudinal conductivity in silicene under the electric field and magnetic field, The European Physical Journal B **92**, 1 (2019).
[48] S. Costamagna, M. Neek-Amal, J. Los, and F. Peeters, Thermal rippling behavior of graphane, Physical Review B **86**, 041408 (2012).
[49] M. Farjam and H. Rafii-Tabar, Comment on "band structure engineering of graphene by strain: First-principles

calculations", Physical Review B **80**, 167401 (2009).
[50] G. Grosso and G. P. Parravicini, *Solid state physics* (Academic press, 2013).
[51] G. Li and E. Y. Andrei, Observation of landau levels of dirac fermions in graphite, Nature physics **3**, 623 (2007).
[52] L.-J. Yin, S.-Y. Li, J.-B. Qiao, J.-C. Nie, and L. He, Landau quantization in graphene monolayer, bernal bilayer, and bernal trilayer on graphite surface, Physical Review B **91**, 115405 (2015).